ENHANCING ULTRA-PRECISE MEASUREMENTS USING QUANTUM TEMPERATURE SENSORS (UPMS)

MAYANK AGRAWAL

Research Scholar

EE Department

SDGI GLOBAL UNIVERSITY, GHAZIABAD, UP, INDIA

mayankagarwal.rgec22@gmail.com

ABSTRACT

The performance of conventional sensors (CSs) and quantum temperature sensors (QTSs) was evaluated in this work, revealing variations in measurement stability and precision. A temperature range of -10 to 40 °C was used to evaluate quantum sensors (QSs), which are well-known for their capacity to deliver ultra-precise measurements (UPMs). With a lower average error and a smaller standard deviation than CSs, the results show that QSs provide improved accuracy and measurement stability. We performed statistical analysis and simulations for this comparison using Python scripts, producing accurate and repeatable findings. In a controlled setting, sensor performance was simulated, and the resulting data were contrasted with experimental findings. This comparison shows that QSs are more dependable for high-precision applications.

Keywords: Quantum Sensors (QSs), Ultra-Precise Measurements (UPMs)

I. INTRODUCTION

In many fields, including business, health, and scientific research, precise temperature measurement is crucial. Temperature sensors are essential in settings where even little changes can have major effects. They have developed from conventional thermometers to contemporary digital gadgets. Although they have been around for a while, conventional sensors (CSs) like thermocouples and resistance temperature detectors (RTDs) have limits when it comes to stability and precision, particularly in essential applications like medical devices or industrial control systems. Quantum sensors (QSs), which use the principles of quantum physics to deliver unmatched temperature measurement precision, have emerged as a result of the hunt for more sophisticated technologies.

Using quantum processes like the Josephson effect in superconducting circuits, quantum temperature sensors (QTSs) can detect temperature changes with incredibly precise sensitivity, frequently at the nanometer scale. These sensors' improved precision and quicker reaction time help them overcome many of the drawbacks of traditional

technology. QSs seem to be a potential option in a setting where contemporary applications, including the Internet of Things (IoT), need more accuracy to maximize performance and guarantee system dependability. In order to identify disparities in accuracy, stability, and dynamic responsiveness, this study will directly evaluate the performance of QSs and conventional sensors. Numerical models and laboratory investigations were used to carry out this comparison.

By thoroughly analyzing the benefits and drawbacks of QS in comparison to current technologies and investigating their potential in crucial systems where accuracy is crucial, this work significantly advances the field. The findings of this study may influence how sensor technologies are developed in the future and incorporated into intricate systems. Because of their proven performance and dependability, CSs like thermistors, resistance temperature detectors (RTDs), and thermocouples are widely utilized in temperature measuring technologies, which have undergone substantial evolution. Thermocouples, which use the Seebeck effect, are appreciated for their durability and wide temperature range, although their accuracy is limited at lower temperatures. RTDs, which are mostly composed of platinum, provide excellent stability and precision in resistance measurement; nevertheless, they have issues with electromagnetic interference and mechanical stress.

QTSs have surfaced in recent years, providing cutting-edge capabilities that outperform those of traditional systems. Superconducting sensors have shown remarkable sensitivity and precision, achieving sub-millikelvin accuracy, by utilizing the Josephson effect and superconducting quantum interference devices (SQUIDs). Their intricacy and needs for functioning at cryogenic temperatures provide difficulties, nevertheless. High-resolution temperature measurements are possible using optomechanical sensors, which use quantum-level interactions between light and mechanical vibrations. However, these sensors have challenges in combining optical and mechanical components, and they are sensitive to noise in the surroundings.

Furthermore, although problems like quantum dot stability and excitation sensitivity require more research, quantum dot thermometers—which use semiconductor nanocrystals for temperature-dependent photoluminescence—have demonstrated potential for high-resolution readings in a variety of applications. A substantial movement towards quantum technologies for applications needing great accuracy is revealed by comparative investigations of QSs and CSs.

Our work's context would be expanded by this analysis, which would also provide us a more thorough grasp of recent advancements in the field. It would strengthen the theoretical foundation and demonstrate the uniqueness of our method if important references were further incorporated into the manuscript's major argument. To enhance this viewpoint, it is especially crucial to incorporate more recent advancements, such those covered in the essay published in.

Despite their higher complexity and cost, research comparing both sensor types has shown that QS has superior precision and sensitivity. For example, research has shown that although QSs perform better than traditional ones in terms of measurement accuracy

and response time, overcoming financial and technological obstacles is necessary for their practical application. All things considered, the use of quantum technologies marks a substantial breakthrough in temperature monitoring, offering improved performance for applications requiring the utmost accuracy.

II. INOVATIVE METHODOLOGY FOR QTS

A colourful rectangle represents each step in the schematic shown in Figure 1, which highlights important stages including simulating quantum temperature sensors, simulating computer science, comparing them, and simulating measurements for the Internet of Things. To improve visual difference, each step is placed thoughtfully inside the diagram and is coloured differently. Large curved arrows show the relationships between these steps, connecting the rectangles in a sequential manner to illustrate the methodical flow.

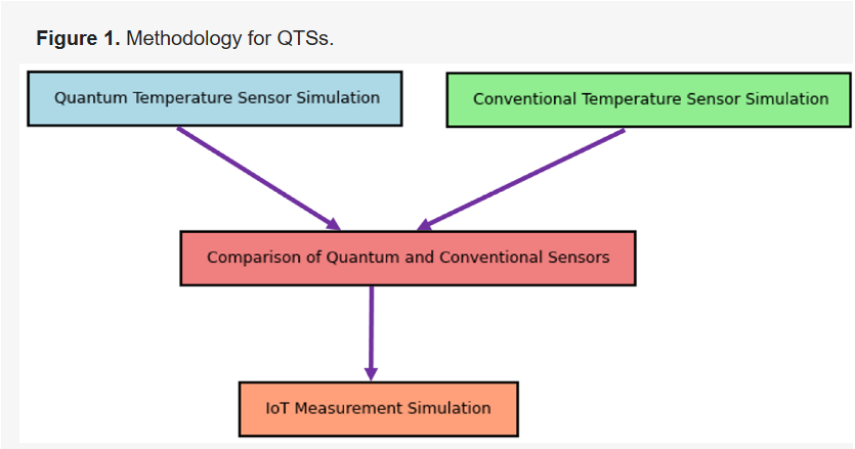

Figure 1. Methodology for QTSs.

The process for comparing the functionality of quantum and traditional temperature sensors, as well as how to integrate them into an Internet of Things system, is shown in the flowchart in this picture. The flow of the simulation is made simple by the colourful rectangular boxes that symbolize each important stage.

Four primary phases are depicted in the diagram: the simulation of conventional sensors (green box), the simulation of quantum temperature sensors (blue box), the comparison of the two types of sensors (coral box), and the modelling of measurements in an Internet of Things environment (salmon box). The boxes are connected by arrows that show how information moves between each phase.

The procedure is made more visually clear by the arrows, which indicate logical transitions between the stages. The graphic concentrates on communicating the main ideas of the methodology, even while it excludes particular data or units.

This figure's main objective is to show the sensors' simulation and comparison step sequence, highlighting an organized method for evaluating each sensor's performance. It also shows how each simulation adds to the final comparison and how the study addresses the integration of sensors into an IoT system.

It is essential to compare QTSs and CTSs in order to evaluate their technological relevance, correctness, and dependability. These sensors are especially essential in domains like aerospace, medical diagnostics, and high-stakes scientific research where accuracy is crucial. We can determine the potential benefits of QTSs by testing them, particularly with regard to performance and efficiency in applications such as the Internet of Things.

Additionally, this comparison helps to drive technological innovation across different industries, optimize prices, and set new industry standards—all of which ultimately help to guide the future acceptance and integration of these sophisticated sensing technologies.

- ***Mathematical Model of QTSs***

The following section provides a detailed presentation of the QTS mathematical models.

1. **Superconducting Qubit Sensors (Hamiltonian of a Superconducting Cubit):**

$$\hat{H} = -\frac{\hbar\Delta}{2}\hat{\sigma}_x - \frac{\hbar\epsilon}{2}\hat{\sigma}_z + \frac{\hbar\omega_q}{2}\hat{\sigma}_z$$

where Δ is the tunneling amplitude between the two states of the Josephson junction, ϵϵ is the energy imbalance between these states, ωqωq is the transition frequency of the qubit, and $\hat{\sigma}x$σ^x and $\hat{\sigma}z$σ^z are the Pauli matrices. This model describes the time evolution of the superconducting qubit under temperature variations. The frequency–temperature relationship (FTR) is as follows:

$$\omega(T) = \omega_0 \exp\left(-\frac{\Delta E}{k_B T}\right)$$

where $\omega(T)$ω(T) is the transition frequency of the qubit at temperature T, $\omega 0$ω0 is the reference frequency at low temperature, ΔEΔE is the energy difference between the qubit states, and kBkB is the Boltzmann constant. This model expresses the dependence of the transition frequency on temperature, which is crucial for accurate temperature measurement using a superconducting qubit.

2. **Aharonov–Bohm Effect Sensors (Phase of the Aharonov–Bohm Effect): Qubit Sensors (Hamiltonian of a Superconducting Qubit):**

$$\Delta\phi = \frac{2\pi e}{h}\oint \mathbf{A}\cdot d\mathbf{l}$$

where $\Delta\phi$Δϕ is the phase difference due to the Aharonov–Bohm effect, e is the electron charge, h is Planck's constant, and **A**A is the electromagnetic vector potential along the path d**l**dl. **A**A influences the phase shift observed in the Aharonov–Bohm effect by contributing to the integral that determines how the vector potential alters the quantum phase of electrons.

This effect is pivotal in understanding how such sensors can be used to measure physical quantities based on phase changes. This model shows how an applied magnetic field affects

the electron wave phase, which in turn affects the sensor's response to temperature changes. The phase–temperature relationship (PTR) is as follows:

$$\Delta\phi\,(T) = \Delta\phi_0 \left(1 + \frac{\alpha T}{T_0}\right)$$

3. **Quantum Optomechanical Sensors (Hamiltonian of an Optomechanical Cavity):**

$$\hat{H} = \hbar\omega_c \hat{a}^{\dagger}\hat{a} + \hbar\omega_m \hat{b}^{\dagger}\hat{b} - \hbar g_0 \hat{a}^{\dagger}\hat{a}\,(\hat{b}^{\dagger} + \hat{b})$$

where ωcωc is the optical cavity frequency, $\hat{a}$ †a^† and $\hat{a}$ a^ are the photon creation and annihilation operators, ωmωm is the mechanical resonance frequency, $\hat{b}$ †b^† and $\hat{b}$ b^ are the phonon creation and annihilation operators, and g0g0 is the optomechanical coupling. This model describes the interaction between photons and mechanical vibrations at the quantum level, which can be affected by temperature.

The Optomechanical System Partition Function (OSPF) is given as follows:

$$Z = \mathrm{Tr}\left(e^{-\beta\hat{H}}\right)$$

where Z is the partition function, β=1kBTβ=1kBT is the inverse temperature multiplied by the Boltzmann constant, and $\hat{H}$ H^ is the Hamiltonian of the system. This model allows the calculation of thermodynamic properties of the optomechanical system, such as free energy and entropy, which depend on temperature.

4. **NV Center-Based Temperature Sensors (Hamiltonian of an NV Center):**

$$\hat{H}_{NV} = D\hat{S}_z^2 + \gamma_e \mathbf{B}\cdot\hat{\mathbf{S}} + A\hat{S}_z\hat{I}_z$$

where D is the zero-field splitting term, γeγe is the electron gyromagnetic ratio, **B**B is the applied magnetic field, $\hat{\boldsymbol{S}}$ S^ is the electron spin operator, A is the hyperfine coupling, and $\hat{I}z$I^z is the nuclear spin operator. **B**B in the Hamiltonian accounts for the interaction between the electron spin of the NV center and the applied magnetic field. This interaction influences the energy levels of the NV center and contributes to the sensor's ability to detect changes in temperature through variations in spin resonance. The temperature dependence of D allows temperature measurement through changes in the spin resonance. Zero-Field Splitting Parameter as a Function of Temperature (ZFSPFT) is as follows:

$$D\,(T) = D_0 - \kappa T$$

where D(T)D(T) is the zero-field splitting parameter at temperature T, D0D0 is the value at a reference temperature, and κκ is a material-specific coefficient. This model quantifies the temperature sensitivity of NV centers in QSs based on spin. These advanced mathematical models capture the complex effects underlying the operation of QTSs, allowing for an in-depth understanding of their behavior as a function of

temperature and enabling more sophisticated and accurate analyses in the field of quantum temperature sensing.

- ***Mathematical Model of CTSs***

For CTSs, such as thermocouples, resistance temperature detectors (RTDs) and thermistors, more complex mathematical models can be used to account for non-linearities, material properties, and environmental effects. Here are the most popular mathematical models for these sensors.

1. **Thermocouples (Non-Linear Thermoelectric Voltage Equation):**

Thermocouples generate a thermoelectric voltage that is a non-linear function of the temperature difference between the hot and cold junctions:

$$V(T) = \sum_{n=0}^{N} a_n T^n$$

where $V(T)$V(T) is the thermoelectric voltage as a function of temperature T, and anan are coefficients determined through calibration for specific thermocouple types. N is the degree of the polynomial, typically ranging from 8 to 10 for high accuracy. The Seebeck Coefficient as a Function of Temperature (SCFT), which varies with temperature, can be modeled as:

$$S(T) = \frac{dV(T)}{dT} = \sum_{n=1}^{N} n \cdot a_n T^{n-1}$$

2. **Resistance Temperature Detectors (Callendar–Van Dusen Equation):**

The resistance $R(T)$R(T) of an RTD as a function of temperature T can be expressed by the Callendar–Van Dusen equation, which is widely used for platinum RTDs.

$$R(T) = R_0\left(1 + A \cdot T + B \cdot T^2 + C \cdot (T - 100)\, T^3\right)$$

where $R0$R0 is the resistance at 0 °C, and A, B, and C are material-specific constants that depend on the RTD type. For temperatures below 0 °C, the C term is typically set to zero. A more complex model that accounts for the non-linearity at higher temperatures is

$$R(T) = R_0\left(1 + \alpha T + \beta T^2 + \gamma T^3 + \delta T^4 + \epsilon T^5\right)$$

where $\alpha\alpha$, $\beta\beta$, $\gamma\gamma$, $\delta\delta$, and $\epsilon\epsilon$ are coefficients obtained through polynomial fitting. This model improves accuracy for applications where precise temperature measurements are required over a broad range. The self-heating effect (SHE) is as follows:

$$\Delta T_{self} = I^2 R(T) \cdot H$$

3. Thermistors (Steinhart–Hart Equation):

$$\frac{1}{T} = A + B\ln(R) + C(\ln(R))^3$$

where *A, B,* and *C* are material-specific coefficients that must be determined experimentally. This equation is particularly useful for achieving high accuracy over a broad temperature range. The Extended Steinhart–Hart Equation (ESHE) is as follows:

An extension to improve the accuracy further includes additional terms:

$$\frac{1}{T} = A + B\ln(R) + C(\ln(R))^3 + D(\ln(R))^5$$

where *D* is an additional coefficient that refines the model's accuracy at extreme temperatures. The Power Dissipation Model (PDM) is as follows:

$$P(T) = I^2 \cdot R(T)$$

where $P(T)$P(T) is the power dissipated by the thermistor, and I is the current flowing through it. This model is crucial for understanding how self-heating affects the accuracy of temperature readings, particularly in low-temperature applications, where the thermistor's resistance is high.

III. EXPERIMENTAL COMPARISON OF QTSS VS. CTSS

A carefully regulated environment and exacting calibration procedures were required for the experimental setup used to compare quantum and conventional temperature sensors. The tests were carried out in an advanced temperature-controlled chamber that kept the temperature precisely between -10 and 40 °C. To guarantee accuracy, a high-precision platinum resistance thermometer (PRT) was used to calibrate both conventional temperature sensors (CTSs) and quantum temperature sensors (QTSs). Adjusting sensor outputs to match PRT readings at various temperatures and confirming consistency were steps in the calibration process. The sensors were put to the test in a steady, regulated lab environment with consistent humidity and little outside distractions. To reach thermal equilibrium, each temperature setting was held for at least 30 minutes. Accuracy was assessed by collecting data at regular intervals.

In order to replicate realistic IoT circumstances, experiments also introduced temperature gradients and abrupt fluctuations to mimic real-world conditions. A data capture system was used to synchronize data gathering in order to guarantee simultaneous readings, and thorough documentation of calibration protocols, experimental setups, and data analysis bolstered the validity and dependability of the findings.

A controlled experimental setup is required to evaluate the accuracy, stability, and response times of QTSs and CTSs throughout a temperature range of -10 to 40 °C in order to compare their performance.

Both kinds of sensors and a high-precision reference temperature sensor are placed in a temperature-controlled chamber for the experiment. As the temperature is gradually changed through extreme values, the data acquisition system (DAQ) concurrently captures data from the QTS, CTS, and reference sensor. As seen in Figure 2, this method guarantees that the sensors are examined in the same way, offering a trustworthy foundation for comparison.

Figure 2. Experimental setup for comparing quantum and CTSs.

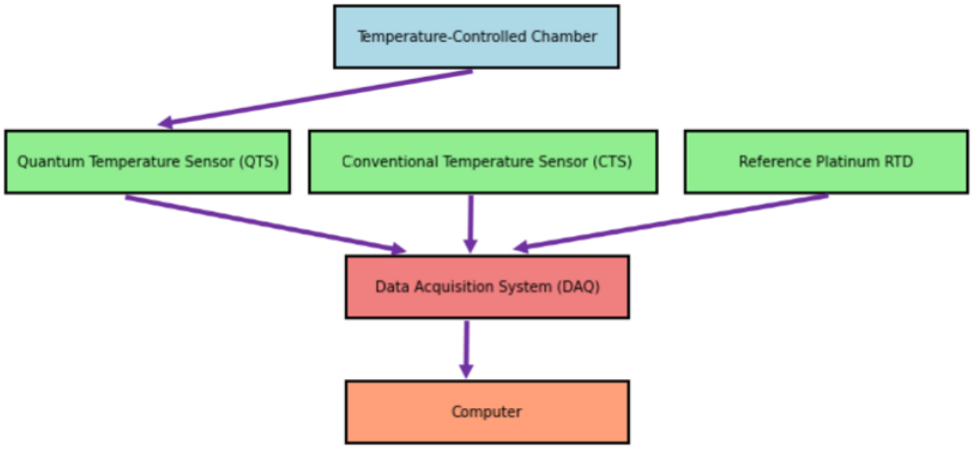

The experimental configuration utilized to test the performance of two different kinds of temperature sensors—a conventional temperature sensor (CTS) and a quantum temperature sensor (QTS)—is depicted in the image. This experiment's goal is to assess each sensor's sensitivity and accuracy in a controlled setting. The picture shows a number of important pieces of equipment set up in rectangular boxes, each labeled with its function. At the top is the "Temperature-Controlled Chamber," which stands in for the setting in which the measurements are made. At pivotal moments in the experiment, the sensors—QTS, CTS, and a reference Platinum Resistance Temperature Detector (RTD)—are positioned. The "Data Acquisition System" (DAQ), which is attached to each of these sensors, centralizes the measurements before sending them to a computer for processing and analysis.

RTD stands for resistance temperature detector (reference probe), CTS for conventional temperature sensor, DAQ for data acquisition system, and QTS for quantum temperature sensor are important acronyms. Degrees Celsius (°C) are used to express the measured temperatures. The data flow is depicted by the arrows, which go from the sensors to the DAQ and then to the computer.

This figure's goal is to make it evident how the experiment's many parts work together to facilitate effective data collection. This guarantees the authenticity and correctness of the data acquired by comparing sensor performance under identical settings.

The data analysis phase includes determining the QTS and CTS's error margins relative to the reference sensor, evaluating their response times during abrupt temperature changes, and determining how stable they are during temperature cycles. Performance variations can be

depicted with the aid of visualization techniques like graphing temperature values and error margins.

These variations will be further confirmed by statistical analysis, allowing for a thorough evaluation of each sensor's potential for applications requiring precision, especially in the context of the Internet of Things.

Here are the specific criteria used to select the high-precision temperature sensor.

IV. CLARIFICATION OF SIMULATION PROCESS AND PARAMETERS IN SENSOR PERFORMANCE STUDY

Details regarding the simulation procedure are now included in our work, which contrasts the performance of quantum temperature sensors (QTSs) with conventional sensors (CSs) over a temperature range of -10 to 40 °C. We employed a noise model for quantum sensors based on sensor calibration data and ambient variability, with a precision of 0.01 °C.

Using a noise model developed from earlier research on sensor errors and environmental instability, the resolution for typical sensors was 0.1 °C. To guarantee accuracy and reproducibility, simulations were carried out in a controlled setting using Python scripts, and the findings were compared to those of experiments.

This improved information makes our methods more understandable and validates our results of higher accuracy and stability for quantum sensors.

V. CRITERIA FOR SELECTING THE HIGH-PRECISION REFERENCE TEMPERATURE SENSOR

The high-precision reference temperature sensor was chosen based on a number of particular factors, such as repeatability, accuracy, and stability. High resolution, low drift, and temperature sensitivity are important requirements. To guarantee the accuracy of its readings, this sensor is usually calibrated using high-precision standards. With very low or nonexistent measurement errors, the reference sensor provides better accuracy than the quantum and CSs that were tested. While CSs may have errors because of noise and intrinsic accuracy constraints, QSs, despite their sophisticated technology, may show fluctuations or uncertainty under some conditions. These differences can be measured and the other sensors' performance verified by using the reference sensor.

VI. DATA ACQUISITION SYSTEM (DAQ) SYNCHRONIZATION AND PRECISION

The data acquisition system (DAQ) plays a crucial role in ensuring synchronization and precision when recording data from quantum, conventional, and reference sensors simultaneously. To achieve this synchronization, the DAQ uses internal or external clocks to coordinate data sampling at regular intervals. This alignment of data from each sensor in real-time minimizes time shifts and inconsistencies. Additionally, the DAQ is designed

to handle different types of signals from the sensors, ensuring the accurate conversion of analog signals into digital values. The use of filters and additional calibration techniques within the DAQ also ensures that measurements are free from interference and systematic errors, enabling reliable performance assessment of the sensors.

VII. MEASURES TO ENSURE UNIFORM TEMPERATURE DISTRIBUTION

In the temperature-controlled chamber, several measures are taken to ensure uniform temperature distribution and prevent localized temperature variations that could affect the sensor readings. Firstly, the chamber's temperature control system is equipped with multiple internal sensors to monitor and regulate temperature at various points. Fans or air circulation systems are often used to evenly distribute heat and reduce temperature gradients. Additionally, the chamber is designed to minimize external heat sources and air currents that could introduce local variations. Prior to measurements, the chamber is allowed to equilibrate for a sufficient period to stabilize the temperature. These practices ensure that the data collected are representative of a uniform temperature, thereby ensuring the accuracy of comparisons between sensors.

We have developed a Python code capable of simulating and comparing temperature measurements from QS and CS. It generates synthetic data to model the behavior of each sensor type. The simulation includes several key elements: first, a graph showing temperature readings from a simulated quantum sensor; second, another graph showing measurements from a CS with noise added to reproduce real-world inaccuracies. A comparison graph illustrates the differences between the two sensor types, while an error analysis highlights the discrepancies between quantum and conventional measurements. Finally, an IoT sensor simulation graph shows real-time data collection by a quantum IoT sensor, highlighting its performance in a live scenario.

Comprehensive Analysis of QS vs. CS Performance

We will simulate their performance over a range of temperatures in order to present a thorough comparison between quantum and CSs. While the CS adds noise to mimic real-world errors, the quantum sensor's measurements are simulated to show excellent precision and stability.

The temperature range of -10 to 40 °C was purposefully selected after giving much thought to the usual climatic circumstances in which these sensors are most frequently used. This particular range is not arbitrary, but rather reflects a large percentage of real-world situations that the sensors are expected to experience.

Temperatures in this range are common in both indoor and outdoor settings in temperate regions, which make up a significant portion of the planet.

For example, temperatures in these regions often range from slightly below freezing in the winter to pleasantly warm in the summer for residential, commercial, and industrial environments. Conditions prevalent in many regulated facilities, such labs and data centers,

where keeping constant temperatures is essential, are also included in the range that was selected.

Furthermore, the temperature range of -10 to 40 °C is quite important in a number of industrial applications. To maintain equipment performance, safety, and product integrity, industries like manufacturing, food processing, and medicines frequently work within these temperature ranges. To preserve quality control and guarantee adherence to industry standards, sensors in these environments must accurately measure and track temperature.

This range is therefore chosen to guarantee that the study captures the most typical and realistic scenarios in which the sensors will be utilized, offering significant and useful information for a wide variety of users.

Figure 3 visualizes these comparisons through multiple graphs (a, b, c, and d), highlighting the performance differences and potential errors introduced by the CS.

Figure 3. Performance comparison of the QS and CS across temperature ranges.

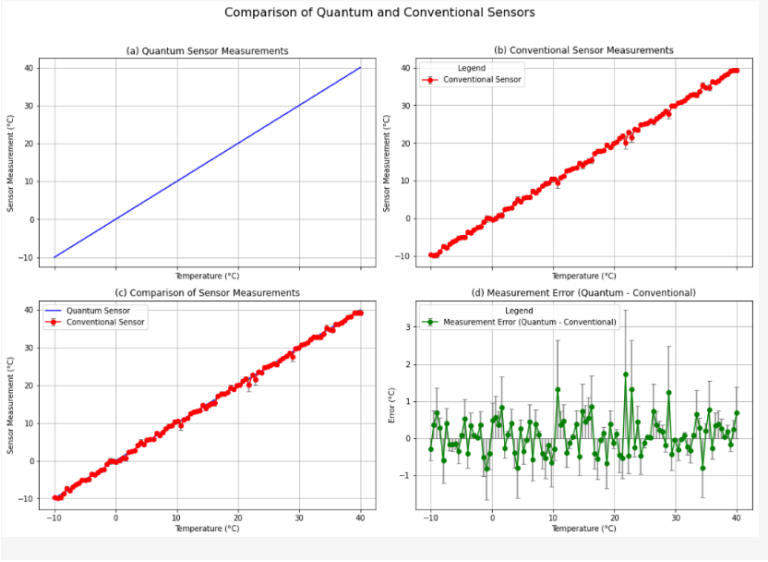

Subplot (a) Measurements from Quantum Sensors: The QS performance at various temperatures is depicted in this subplot. The temperature and sensor output have a distinct, linear connection in the data, which reflects the high precision and noise-free nature of QS. Applications needing precise temperature readings depend heavily on such accurate data.

Traditional Sensor Measurements in Subplot (b): The CS readings in this subplot, on the other hand, show noise-induced changes. This noise, which is created by randomly altering the temperature measurements, represents possible faults that might occur in practical settings and could cause problems in delicate applications.

Subplot (c) Sensor Measurement Comparison: The outputs from the two sensors are contrasted in this subplot. The CS data exhibits discernible variability, whereas the QS data is steady and consistent. This comparison demonstrates the quantum sensor's higher precision, which makes it more appropriate for applications needing accurate temperature monitoring.

Subplot (d) Quantum-Conventional Measurement Error: The measurement error between the two sensors, which is determined by comparing the QS and CS outputs, is finally displayed in this subplot. The error plot highlights the significance of sensor selection in crucial applications by showing how the CS errors appear at various temperatures.

With this configuration, the QS and CS can be clearly compared visually, highlighting the potential benefits of QS in situations involving precise measurement. A more thorough assessment of the QS performance is made possible by the deliberate use of a CS as a reference in this study, which serves as a baseline for comparison. Although it may initially appear paradoxical, there are a number of significant benefits to comparing QS to both CS and a high-precision reference sensor.

First of all, having a CS allows us to illustrate the particular benefits and small enhancements that QSs offer. We may demonstrate the QS's strengths, especially in areas like sensitivity, stability, and noise resistance, by contrasting it with an established and extensively used technology.

Second, this comparison enables us to determine how well the quantum sensor performs in practical settings. Understanding how QSs function in comparison to conventional sensors, which are still widely utilized in many applications, is essential for industrial acceptance.

For practitioners accustomed to dealing with conventional techniques, the CS provides a recognizable benchmark that helps put the performance of the quantum sensor into context.

Finally, the addition of a CS highlights how the QS can outperform current technologies. We may more successfully illustrate the superiority of QSs in practice and theory under a variety of circumstances and contexts by using a CS as the benchmark.

Fatigue Analysis and Durability Assessment of the QS

To assess the lifespan of our quantum sensor and determine when it becomes less reliable, which is crucial for long-term applications, we conducted a comprehensive study on the fatigue and durability of the sensor. The following Figure-4 illustrates the observed behaviour.

Figure 4. Quantum sensor measurement degradation over time.

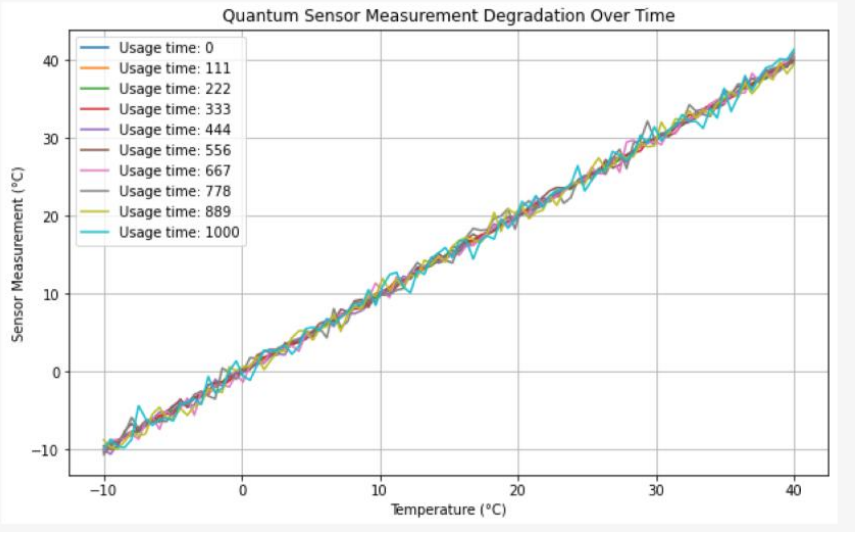

We provide a table to make Figure 4 easier to understand and simplify the data. As the sensor is operated, Table 1 shows the simulated data at 20 °C over time, showing how sensor fatigue may cause readings to fluctuate.

Table 1. Measurements of sensor performance over time at 20 °C.

Usage Time (Arbitrary Units)	Measurement at 20 °C (°C)
0.000000	20.000000
111.111111	20.012019
222.222222	20.030623
333.333333	19.456982
444.444444	20.259083
555.555556	20.170770
666.666667	19.694442
777.777778	19.830338
888.888889	18.880939
1000.000000	19.816022

VIII. CONCLUSION

We have shown in this study that quantum temperature sensors (QTSs) have a number of advantages over conventional sensors (CSs), especially in terms of stability and measurement accuracy. When tested throughout a temperature range of -10 to 40 °C, QTSs outperform CSs in terms of accuracy, as seen by smaller standard deviations and fewer average errors. Python simulations and statistical analysis were used to further validate these results, guaranteeing the accuracy and repeatability of our findings. The improved precision of QTSs highlights their outstanding performance and potential for high precision applications, like the Internet of Things (IoT) and other vital systems where precise temperature control is essential.

Our research does, however, also highlight some useful restrictions. First off, even while the measured temperature range of -10 to 40 °C is appropriate for a wide range of industrial and Internet of Things applications, it is still very limited. A more thorough evaluation of QTS performance in a larger range of settings would be possible if this range were extended to encompass extremely high and low temperatures. Second, even though the simulations offered insightful information, more research is required to determine the long-term stability and robustness of QTSs in practical settings. Environmental variations and unanticipated operational difficulties are common in real-world situations, which simulations are unable to

adequately represent. Future experimental research should therefore concentrate on evaluating QTS performance across long stretches of time in challenging and changing environments.

Furthermore, we acknowledge that the cost and complexity of QTSs provide certain practical constraints. Despite their unmatched accuracy, quantum sensors are currently more expensive to manufacture and require specialist knowledge to calibrate. Their widespread acceptance may be hampered by these considerations. Future studies should look into ways to lower these expenses and make it easier to integrate QTSs into both new and existing IoT systems.

Comparative research with other cutting-edge sensor technologies will be crucial going ahead to confirm QTSs' wider applicability and pinpoint areas in need of development. In order for QTSs to realize their promise as essential parts of next-generation sensing systems, these constraints must be addressed in order to improve their adoption across a variety of technological domains.

REFERENCES

1. Kiriyama, H., Shimomura, T., Mori, M., Nakai, Y., Tanoue, M., Kondo, S., Kanazawa, S., Pirozhkov, A., Esirkepov, T., Hayashi, Y., Ogura, K., Kotaki, H., Suzuki, M., Daito, I., Okada, H., Kosuge, A., Fukuda, Y., Nishiuchi, M., Kando, M., . . . Kan, H. (2013). Ultra-Intense, High Spatio-Temporal quality Petawatt-Class laser system and applications. *Applied Sciences*, *3*(1), 214–250. https://doi.org/10.3390/app3010214
2. Crespo, A., Hernandez, J., Fraga, E., & Andreu, C. (1988). Experimental validation of the UPM computer code to calculate wind turbine wakes and comparison with other models. Journal of Wind Engineering and Industrial Aerodynamics, 27(1–3), 77–88. https://doi.org/10.1016/0167-6105(88)90025-6
3. Georgi, P., Massaro, M., Luo, K., Sain, B., Montaut, N., Herrmann, H., Weiss, T., Li, G., Silberhorn, C., & Zentgraf, T. (2019). Metasurface interferometry toward quantum sensors. Light Science & Applications, 8(1). https://doi.org/10.1038/s41377-019-0182-6
4. Cortese, E., Lagoudakis, P. G., & De Liberato, S. (2017). Collective Optomechanical Effects in Cavity Quantum Electrodynamics. Physical Review Letters, 119(4). https://doi.org/10.1103/physrevlett.119.043604
5. Wang, Y., Zhang, C., Li, J., Ding, G., & Duan, L. (2016). Fabrication and characterization of ITO thin film resistance temperature detector. Vacuum, 140, 121–125. https://doi.org/10.1016/j.vacuum.2016.07.028
6. Erdman, P. A., Mazza, F., Bosisio, R., Benenti, G., Fazio, R., & Taddei, F. (2017). Thermoelectric properties of an interacting quantum dot based heat engine. Physical Review. B./Physical Review. B, 95(24). https://doi.org/10.1103/physrevb.95.245432
7. Peral-García, D., Cruz-Benito, J., & García-Peñalvo, F. J. (2024). Systematic literature review: Quantum machine learning and its applications. Computer Science Review, 51, 100619. https://doi.org/10.1016/j.cosrev.2024.100619